ISSN 0001-4370, Oceanology, 2015, Vol. 55, No. 4, pp. 644–656. © Pleiades Publishing, Inc., 2015.
Original Russian Text © A.G. Rozanov, 2015, published in Okeanologiya, 2015, Vol. 55, No. 4, pp. 709–722.

MARINE GEOLOGY

Geochemical Features of the Deepwater Sediments of the Kara Sea (Novaya Zemlya Basin and St. Anna Trench)

A. G. Rozanov

Shirshov Institute of Oceanology, Russian Academy of Sciences, Moscow, Russia

e-mail: rozanov@ocean.ru

Received February 12, 2014; in final form, March 31, 2014

Abstract—The northwestern part of the Kara Sea is peculiar in its rugged topography, represented by the Novaya Zemlya Basin and St. Anna Trench, where almost no river runoff enters. These closely spaced seafloor basins differ in sedimentation conditions, source of sedimentary material, and properties of bottom sediments, the geochemical features of which, in particular redox properties, are presented in this paper.

DOI: 10.1134/S0001437015030145

INTRODUCTION

The main factor of sedimentation in the Kara Sea is the influx of terrigenous material as particulate matter with rivers from the south (Ob and Yenisei rivers) (95%) [9] and with sea currents from the north and west (Barents Sea). The mixing of seawater and fresh water resulted in the complex and ambiguous dynamics of the Kara Sea, which shows seasonal and annual variations depending on ice setting, climatic changes, and related values of the river runoff. In studying the Kara Sea, main attention was given to fresh- and seawater mixing and corresponding frontal zones where these processes are best expressed. In this work, we consider the geochemical features of sedimentation and diagenesis of deepwater sediments, in particular, the sediments of the Novaya Zemlya Basin (NZB) and the St. Anna trench (SAT), which are located far from the mixing region (Fig. 1).

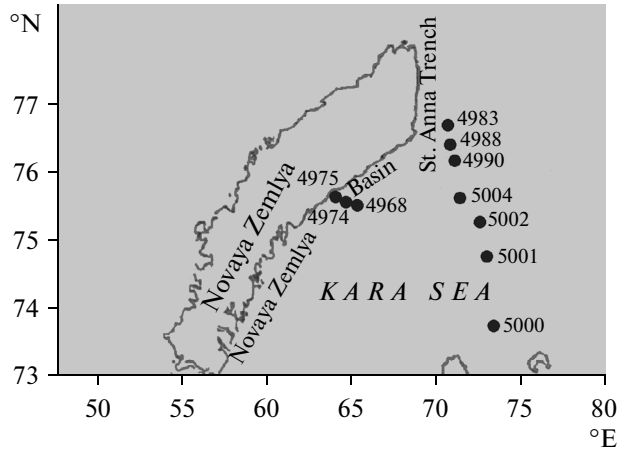

Fig. 1. Map of geochemical stations made in the Novaya Zemlya Basin and St. Anna Trench (stations considered previously [13] are noted by lighter type).

MATERIALS AND METHODS

Bottom deposits were sampled during Cruise 54 of R/V *Akademik Mstislav Keldysh* in 2007 [18] using bottom grabs and geological pipes, including a Niemiste corer, which allowed simultaneous sampling of small amounts of the bottom water above sediment. The moisture of sediments was determined by air drying up to constant weight at 105°C. Redox potential (E_{Pt}) was measured using platinum electrodes [13]. Pore water were separated from sediment by centrifuge. After filtration through membrane filters (Millipore, 0.45 μm), pore water were analyzed for dissolved inorganic species of manganese (with formaldoxyme), iron (with ferrozine), phosphates, and silica acid [13]. Chemical elements in the solid phase of a sediment were determined by atomic absorption flame spectroscopy in dry samples after acid digestion ($HF + HClO_4$) (Table 1).

RESULTS

The studies were carried out in the *Novaya Zemlya Basin (NZB)*, located in the vicinity of the Novaya Zemlya islands, near Blagopoluchiya Bay, and reaching a depth of 360 m. The hydrological profile of the basin, from top to bottom, consists of a 10-m stirred layer, sharp thermocline, a 20–50 m cold transitional layer (CTL, –1.7°C), and a layer of warmer water (–0.8°C), whose temperature monotonously decreases down to the seafloor (–1.5°C). It is suggested that the deep water of the NZB is formed under the effect of cold and saline waters sinking from the Novaya Zemlya shelf during active ice formation [5]. In contrast, the Upper Convective Layer (UCL) is formed during thawing of the Novaya Zemlya ice mas-

Table 1. Geochemical characteristics of the bottom sediments (%) and pore water (μM) of the Novaya Zemlya basin and St. Anna trench (northwestern Kara Sea)

Sampling tool	Horizon, cm	Description of sediment	E_{Pt}, mV	H_2O	C_{org}	$CaCO_3$	Al	Fe	Mn	Fe	Mn	P	Si
				%						μM			
Novaya Zemlya Basin, the Blagopoluchiya Bay area													
Station 4968. 75°23.3′ N, 64°18.8′ E. Axial part. The depth is 360 m													
NC	15 cm	Water above sediment								0.01	0.1	0.68	16.3
	5 cm	The same. More turbid										0.63	18.6
	0–5	Brown soft over the entire core, with micronodules in the surface horizons (FMN)	+604	64.1	0.96	1.10	7.09	4.70	0.063	0.01	0.1	0.35	249
	5–10		+582		1.02	1.03	8.26	6.03	1.020	0.01	4.7	0.10	226
	10–15		+541				8.13	5.89	0.989	0.01	83.4	3.50	276
	15–20		+526		0.80		8.17	5.96	0.954	0.01	126	3.04	223
	25–30		+477				7.65	5.45	1.208	0.01	251		
LDC	10–21	Brown silty–claye, with dark interbed at 38–41 cm	+545	60.4	0.80	1.07	8.10	6.75	1.960	0.08	18.6	2.69	209
	25–35		+545	58.3	0.78	0.50	8.60	6.80	1.380	0.01	73.0	2.80	249
	35–47		+433	57.5	0.75	0.34	9.15	7.80	2.940	1.25	109	1.63	231
	50–58	Light gray with brown, very dense clumps	+120	55.8	0.65	5.13	7.60	9.35	0.680	1.79	115	8.52	143
	82–86	Darker, with black films	+60	47.9			8.14	6.32	0.180	0.93	123	0.01	122
	96–125	The same, denser	+30				8.37	6.74	0.052	0.01	141	0.01	141
	141–153	The same, with clumps (FeS)	+40	48.4	0.39	0.25	8.62	6.80	0.190	0.31	82.9	0.58	129
	153–170	Darker, soft	+60		0.42		9.04	5.10	0.056	0.70	77.7	1.63	371
	223–232	The same	+145	35.5	1.05	2.57	8.85	4.94	0.073	0.93	53.9	0.01	90.5
	272–304	Denser (FeS)	+150				7.00	3.78	0.050	0.78	52.6		
	324–345	Very dense, pebble	+160				7.25	3.94	0.05	6.23	19.3		
Station 4974. 75°34′.8 N, 64°09′.3 E. Basin slope. Depth is 170 m													
Bg	0–5	Soft mud, downward denser, gray, with brown tint	+497	43.6	0.85	11.12	7.54	4.93	0.380	0.01	0.1	6.19	499
	5–10		+494	39.6	0.96	9.06	7.68	4.91	0.175	0.01	134	5.61	459
	10–15		+487	38.4	0.96	6.31	7.36	4.71	0.410	0.01	91.8	5.72	221
LDC	10–18	Gray, soft	+455	31.8	0.91	6.15	9.58	5.88	0.181	0.01	36.8	1.87	282
	18–20	Gray with ochreous films, dense, clots	+448										
	20–25	Black clayey	+220								11.3		
	25–32	The same	+136	35.3	1.06	3.47	9.87	4.50	0.051				
	32–61	Gravelly–pebbly (70%)	+60	16.6	1.18	9.13	8.76	3.78	0.094				
	60–85	Black hydrotroilite	+80	19.0	1.14	14.19	8.95	4.34	0.150	0.01	2.33		

Table 1. (Contd.)

Sampling tool	Horizon, cm	Description of sediment	E_{Pt}, mV	H_2O	C_{org}	$CaCO_3$	Al	Fe	Mn	Fe	Mn	P	Si
				%						μM			
Station 4975. 73°38′.7 N 64°03′.9 E. Shelf near the basin. Depth is 58 m													
Bg	0–5	Gray soft, becomes denser downward, homogenous	+497	33.6	0.68	19.68	8.40	3.08	0.109	0.16	13.0	35.5	188
	5–10		+150	35.9	0.63	19.52	8.70	4.02	0.094	0.01	0.1	0.01	216
	10–15		+130	32.0	0.88	16.37	9.10	4.07	0.077	0.01	83.2	0.01	239
LDC	10–24	Gray, darkened with depth, numerous pebbles at 24–42 cm	+30	27.7	1.50	14.62	8.86	4.28	0.071	0.01	59.1	0.01	175
	24–42		+74	19.0	1.31	10.71	9.30	4.48	0.088	0.01	42.6	0.01	131
	42–59		+80	24.5	1.21	10.37	8.80	4.42	0.088	0.01	53.9	0.01	262
St. Anna trench (southern part)													
Station 4983. 76°55′.5 N, 70°17′.8 E. The depth is 550 m													
NC	0–4	Brown–gray, semiliquid	+310	71.3	1.62	0.54	8.70	4.60	0.112	0.08	22.6	3.97	320
	4–8	Gray, locally ochreous, dense, polychaete tubes	+140	53.5	1.43	0.59	8.90	4.53	0.038	0.01	4.32	1.87	126
	8–15	The same, denser	+150							0.01	1.33		
LDC	5–9	Gray, semiliquid	+100	48.9	1.40	0.41	9.10	4.24	0.037				
	9–13	Denser, ochreous, with inclusions, clumpy	+150	49.2	1.49	0.41	9.01	4.38	0.038	4.67	6.6		
	20–30	Denser, HT traces, much gas (methane), cavities	+80	47.2	1.67	0.41	9.15	6.79	0.038	0.01	0.1		
	80–90	The same	+64	44.9	0.99	3.00	8.45	3.70	0.038	0.01	5.0		
	115–125	The same, lesser gas	+60	45.0	1.30	1.07	8.50	4.28	0.039	0.01	3.7		
	150–160	Elevated content of HT	+100	42.9	1.21	0.41	8.70	4.53	0.041	0.01	8.3		
	179–184	Lighter with ochreous interbed, watered	+40	35.3	0.55	0.59	7.63	4.24	0.047	0.01	11.3		
	184–206	Dark gray, very dense clay, with pebbles	+100	22.4	0.52	0.84	6.35	2.84	0.054				
Station 4988. 76°35′.3 N, 71°15′.4 E. Depth is 180 m													
Bg	0–2	Gray-brown, semiliquid, with numerous organisms	+494	42.8	0.58	1.16	6.20	4.44	0.135	0.01	0.1	1.17	282
	2–5	Soft, gray	+180	39.6	0.54	2.00	6.15	4.39	0.068	0.16	55.4	0.82	194
	5–10	Gray, denser	+40	35.5	0.56	0.50	6.00	3.80	0.037	2.49	15.5	0.01	143

Table 1. (Contd.)

Sampling tool	Horizon, cm	Description of sediment	E_{Pt}, mV	H_2O	C_{org}	$CaCO_3$	Al	Fe	Mn	Fe	Mn	P	Si
				%						μM			
LDC	10–22	Ochreous, semidry clumps, light plates ($CaCO_3$?)	+190	28.5	0.52	1.91	9.25	4.87	0.041	0.01	0.1	0.01	96.7
	22–33	Watered, with inclusions of coarse silt	+25	20.9	0.23	1.57	4.30	2.0	0.024	0.01	0.1		20.9
	33–45	Dense, dark gray	+100	23.2	0.39	1.07	5.65	2.85	0.036	0.46	0.1		
	70–80	The same	+2	18.3	0.30	1.41	5.47	2.94	0.040		0.1		
	90–100	The same	+110	18.5	0.27	2.32	5.41	3.28	0.064				
	106–123	Very dense dark gray clay with silt	+70	18.6	0.33	1.57	5.55	1.91	0.040				
Station 4990. 76°09′.0 N, 72°29′.7 E. The depth is 114 m													
NC	0–3	Brown liquid	+576	45.3	0.47	2.00	6.70	5.23	0.910	0.16	0.1	0.47	322
	3–8	Gray, denser, with ochreous inclusions	+70	41.2	0.48	0.75	6.92	4.77	0.067	0.16	59.6	0.01	220
	8–15	Gray, dense	+45	41.9	0.42	0.56	6.75	4.30	0.050		42.4	0.01	172
LDC	20–40	The same, with films of HT in the lower part	+60	34.9	0.41	0.50	6.78	3.89	0.053	1.26	80.5	0.01	132
	40–105	The same with maximum amount of HT, horizon of 40 cm is watered	–20	35.8	0.54	0.34	7.52	5.04	0.054	0.16	33.3	0.01	174
	105–123	The same	+40	40.5	0.47	1.50	7.50	5.45	0.058	0.01	27.0		
	123–170	The same, less HT	+170	39.2	0.45	0.82	8.12	5.70	0.060		22.1		
	170–186	Dense, with scarce black spots of HT	+40	36.8	0.48	1.41	7.40	8.13	0.057		10.6		
	196–206	Brown with green tint and clear boundary	+110	26.7	0.52	0.75	7.10	3.54	0.032	0.01	4.88	1.40	299
	206–216	The same, less dense	+180	21.9	0.39	0.16	6.40	2.97	0.038	0.01	95.2	0.01	311
	222–235	The same	+160	20.3	0.27	0.16	6.42	2.85	0.043	0.01	13.3	0.01	304

(Bg) bottom grab sampler, (NC) Hydrostatic Corer, (LDC) Large Diameter Corer, (HT) hydrotroilite, (FMN) ferromanganese nodules.

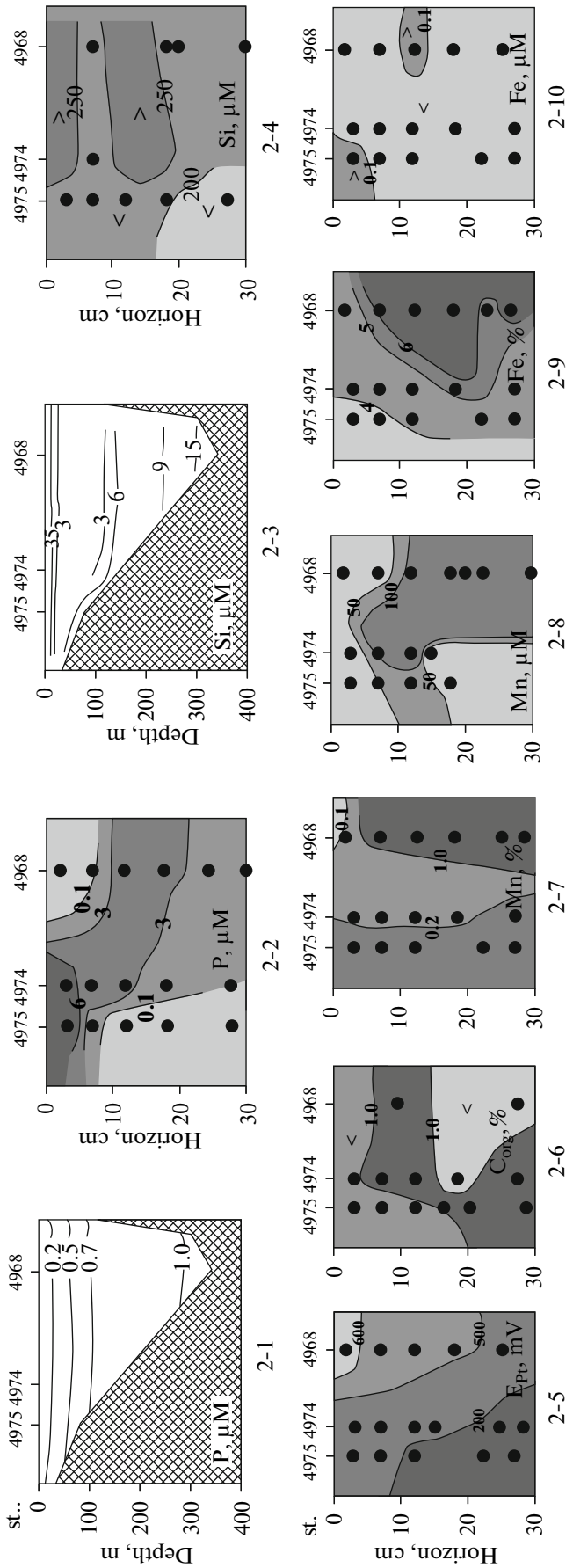

Fig. 2. Geochemical parameters of seawater and bottom sediments of the Novaya Zemlya Basin in the area of Blagopoluchiya Bay: dissolved inorganic species of phosphorus ($P\text{-}PO_4^{3-}$) and silicon ($Si\text{-}SiO_4^{4-}$) in seawater (2-1 and 2-3) and pore water (2-2 and 2-4), μM, the values E_{Pt}, (mV) 2-5, C_{org} 2-6, manganese 2-7, and iron 2-9 in bottom sediments (% of seawater) and in pore water (μM) 2-8 and 2-10, respectively.

sif and the westward influx of the desalinated Yenisei and Ob waters. The intense NE-directed Novaya Zemlya current exists along the coast and deepens seaward. The SW-directed counter-current was identified at a depth more than 100 m on the western slope of the basin on the basis of geostrophic calculations. Complex hydrodynamics suggests that sedimentary material was supplied into the NZB as from the Novaya Zemlya archipelago and with the fresh water runoff from the east and with the Barents Sea from the north and south.

Already in the CTL, surface waters acquire high salinity (34.5 PSU), which only slightly increases with depth (34.7 PSU). Other parameters, in particular hydrochemical characteristics, show wide variability, especially in the top 100 m (Table 2, Fig. 2) [10]. Surface waters differ in their high oxygen saturation, but are low in biogenic elements, except for silica and pH, which reached maximum values in this region. In the subsurface waters, in the thermocline and CTL, the content of dissolved silica sharply decreased and gradually increased to the bottom (Figs. 2–3). Judging from silica distribution throughout this section (Fig. 1) and other hydrochemical parameters obtained at the adjacent stations [10], the deepest water station 4968 is the boundary between waters of the western and eastern parts of the basin.

A surface lens of highly desalinated waters with salinity in its core of less than 18 PSU, temperature of 4.5–4.9°C, and area of 19 thousand km^2 was found during studies near the Novaya Zemlya eastern coast [5]. The lens was formed in June during the Ob and Yenisei floods and was carried to the Novaya Zemlya Islands by northeastern winds. This lens was mainly composed of the Yenisei River waters, the runoff of which is over two times higher than that of the Ob River, which was confirmed by analysis of the relationship between the salinity, alkalinity, and dissolved silica [10]. The upper homogenous part of the lens (8–15 m) was underlain by a 2–3 m high-gradient layer with the salinity gradient of 4.5–6.2 PSU and temperature of 1.4–2.4°C per one meter. As seen from previous data, the concentration of dissolved silica in this layer decreased by more than an order of magnitude (Table 2, Figs. 2–3). Biological studies [11, 17] revealed the inhomogeneity of the lens: its upper part, dominated by diatom algae, provides high values of population, biomass, and chlorophyll *a* (chl *a*), which are 2–3 times lower in the lower dinoflagellate-domi-

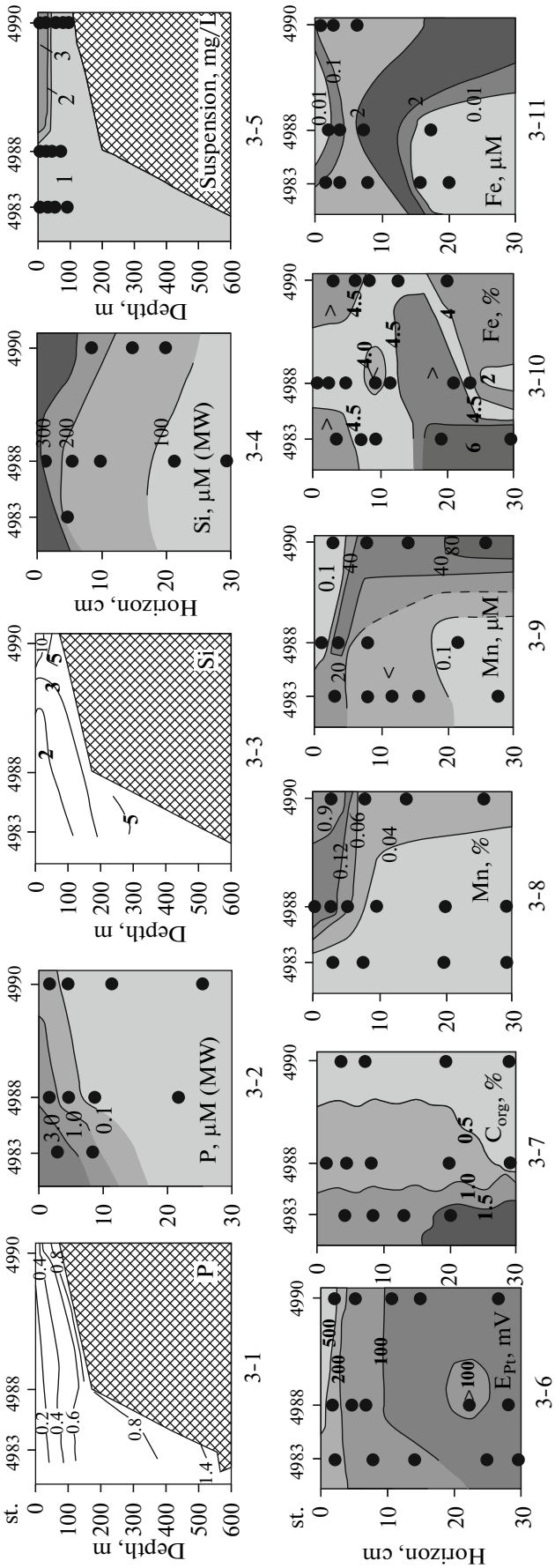

Fig. 3. Geochemical parameters of seawater and bottom sediments of the St. Anna Trench (southern part): dissolved inorganic species of phosphorus ($P\text{-}PO_4^{3-}$) and silicon ($Si\text{-}SiO_4^{4-}$) in seawater and pore water (μM): 3-1, 3-3, and 3-2, 3-4, respectively, suspension in sea water (mg/L) 3-5, E_{Pt} (mV) 3-6, C_{org} 3-7 in the bottom sediments (% dry), manganese 3-8, 3-8, and iron 3-10, 3-12 in bottom sediments (% dry) and in pore water (μM), respectively.

nated part. The high concentrations of dissolved silica in the lens and its almost complete absence beneath it may indicate a sufficiently intense silica circulation between water and Si-bearing plankton.

The boundary between the freshened surface waters of the Novaya Zemlya current and the Barents Sea waters propagating from the north is identified by optical methods, according to which the intensity of fluorescence of dissolved OM in the northern waters decreased by 2–4 times, while that of chl *a* decreased by 4–10 times [2]. The concentrations of aliphatic hydrocarbons (AHC) in the Kara Sea open waters are sufficiently low (8 μg/L), and increase to 27.8 μg/L only near the coast in Blagopoluchiya Bay [12], which is obviously related to the effect of freshened lens. The measurements of sedimentary matter near the eastern slope of the Novaya Zemlya Basin (water depth of 130 m) were previously performed using sedimentation traps, which provides insight into sedimentary fluxes at horizons of 60 and 100 m (25 and 52.8 mg/m^2 per day, respectively, at C_{org} flux of 5.54 and 0.04 mg C/m^2 per day, respectively) [9]. The main part of the sedimentary matter is represented by the pelletes of plankton; the value *f*, representing the fraction of new production of total primary production, was 0.05, which is typical of oligotrophic basins, including the Kara Sea.

The bottom sediments of the NZB are mainly represented by silty–pelitic muds with low $CaCO_3$ content (Table 1). A brown oxidized layer (up to 50 cm thick) was found in the axial deepwater part of the basin (station 4968, depth of 355 m). This layer is thicker than those found at the other stations of the Kara Sea [13, 14]. It is characterized by the maximum E_{Pt} (up to 600 mV) among those measured in the surface sediments of the Kara Sea and by the presence of ferromanganese micronodules. The lower part of the oxidized sediments contains a darker interbed (38–41 cm), where both sediments (up to 3 and 8–9%) and pore water (over 100 and 1.2–1.8 μM, respectively) are enriched in manganese and iron, with brown, very dense clots in the underlying light gray mud (50–58 cm). The obvious reduction (a sharp decrease of E_{Pt}) and partial transition of Mn and Fe in the pore water solution lead to the destruction of the oxidized layer (clots) and redistribution of Mn and Fe along the sedimentary profile. The diagenetic origin of horizons with elevated concentrations of oxidized manganese and iron species is confirmed by their mutual position:

Table 2. Chemical characteristics of seawater in the area of the Novaya Zemlya Islands and St. Anna Trench

Component	Novaya Zemlya area			St. Anna Trench area		
	st. 4975, depth 62 m	st. 4974, depth 170 m	st. 4968, depth 355 m	st. 4983, depth 555 m	st. 4988, depth 183 m	st. 4990, depth 128 m
Salinity, ‰	16.6 (2 m)	15.1 (3 m)	15.7 (2 m)	34.3 (2 m)	33.8 (2 m)	26.3 (2 m)
	32.4 (15 m)	31.0 (15 m)	33.2 (20 m)	34.8 (200 m)	34.4 (82 m)	33.6 (33 m)
	34.5 (60 m)	34.6 (135 m)	34.7 (350 m)	34.9 (528 m)	34.8 (178 m)	34.3 (111 m)
O_2 mL/L (% of saturation)	8.05 (98.9)—2 m	8.01 (98.6)—3 m	8.18 (100.8)—3 m	7.74 (101.2)—2 m	7.51 (98.7)—2 m	8.04 (98.5)—2 m
	7.19 (86.9)—60 m	7.25 (86.8)—135 m	8.09 (106.0)—20 m	7.37 (90.5)—200 m	7.61 (92.1)—82 m	7.85 (92.4)—33 m
			6.41 (76.3)—350 m	7.07 (88.3)—528 m	7.64 (95.3)—178 m	6.92 (83.5)—111 m
pH	8.07 (2 m)	8.05 (3 m)	8.09 (2 m)	8.22 (2 m)	8.16 (2 m)	8.10 (2 m)
	8.06 (60 m)	8.03 (135 m)	8.17 (20 m)	8.07 (200 m)	8.10 (82 m)	8.10 (33 m)
			7.98 (350 m)	7.96 (528 m)	8.11 (178 m)	8.01 (111 m)
Alk (HCO_3^-), mM	1.58 (2 m)	1.55 (3 m)	1.53 (2 m)	2.34 (2 m)	2.31 (2 m)	2.00 (2 m)
	2.36 (60 m)	2.40 (135 m)	2.37 (350 m)	2.37 (200 m)	2.35 (82 m)	2.31 (33 m)
				2.37 (528 m)	2.37 (178 m)	2.34 (111 m)
$N\text{-}NO_3^-$, μM	0.34 (2 m)	0.55 (3 m)	0.45 (2 m)	1.60 (2 m)	1.26 (2 m)	1.51 (2 m)
	6.8 (60 m)	12.9 (135 m)	10.13 (350 m)	10.59 (200 m)	4.69 (82 m)	4.11 (33 m)
				10.15 (528 m)	4.97 (178 m)	9.08 (111 m)
$P\text{-}HPO_4^{2-}$, μM	0.13 (2 m)	0.12 (3 m)	0.13 (2 m)	0.19 (2 m)	0.20 (2 m)	0.29 (2 m)
	0.77 (60 m)	0.88 (135 m)	1.05 (350 m)	0.74 (200 m)	0.53 (82 m)	0.50 (33 m)
				1.40 (528 m)	0.59 (178 m)	0.80 (111 m)
$Si - H_4SiO_4$, μM	36.9 (2 m)	38.1 (3 m)	36.7 (2 m)	1.03 (2 m)	1.18 (2 m)	17.5 (2 m)
	7.4 (60 m)	8.37 (135 m)	1.53 (20 m)	3.68 (200 m)	3.39 (82 m)	3.6 (33 m)
			16.6 (350 m)	6.54 (528 m)	3.27 (178 m)	8.1 (111 m)

the manganese maximum in pore water is located above the iron maximum (Table 1). A less expressed redistribution is also observed in the other horizons of the oxidized layer, as well as in the underlying reduced sediments and in the Upper Pleistocene sediments, which indicates a notable irregularity in sedimentary influx and diagenesis.

The boundary between the Holocene and Upper Pleistocene sediments may be conditionally drawn along the notable coarsening of sedimentary material, the appearance of pebble interbeds, compaction and moisture decrease (up to 35%), which led the authors of [7] to term these rocks "dry clays." Their origin is thought to be related to the rearrangement of the near-bottom circulation during deglaciation and transition to the Holocene [6]. The iron content in reduced sediments remains high (6–7% at the axial station 4968, 80–150 cm), decreasing to less than 4% in the deeper Upper Pleistocene horizons (250 cm). Mn content decreases to background values (0.05%) already in the horizon of 96–126 cm, although sediments with high Mn and Fe contents were found at deeper horizons (Table 1). Similar tendencies are also observed at shelf stations (Table 1, Fig. 2). The manganese content in the pore water also decreases relatively evenly along the profile of sedimentary core, while the iron content shows a drastic drop, which may be related to the uneven sedimentary influx.

The C_{org} content in the surface sediments reaches 1%, which provides the reducing background of the underlying deposits. The main characteristic of this background is the formation of redox stratification in the thermodynamic sequence of OM oxidizers: oxygen, nitrates, manganese and iron oxyhydroxides, sulfates, and carbonic acid [14]. Black films of hydrotroilite are observed at a depth of 80 cm and deeper, while C_{org} decreases along the profile of trench sediments up to 0.4% within approximately 2 m (Table 1, Fig. 2), and inorganic products of the reducing process (CO_2, N_2, Mn^{2+}, Fe^{2+}, S^{2-}, and CH_4) are usually formed in the bottom sediments. The composition of residual OM also shows variations. In particular, AHC determinations revealed that the transition from the surface oxidized sediments to the deeper reduced sediments is accompanied by a change of hydrocarbon concentration in OM, which decreases more rapidly than the concentration of other OM [12]. The lower horizons of sediments from deepwater station 4968 (223–232 cm) demonstrate a jump in C_{org} (1.05%) associated with an increase of content of dissolved iron in the mud waters of the overlying horizons (Table 1). The surface horizons of deepwater sediments, as other sediments of the Kara Sea, contain a few tens of μL/L methane, while its concentrations in sediments from the southern parts of the sea may reach hundreds of μL/L. The methane concentration in the bottom water is close to 1 μL/L, which is related to its oxidation in the water–sediment interface [15].

At station 4974 located on the slope of the basin (170 m) (Table 1, Fig. 2), the oxidized layer has a much lower thickness (20 cm), while ochreous films in the lower part indicate an "iron" redox stage. On the shelf adjacent to the basin (station 4975, depth of 58 m), the thickness of the oxidized layer decreases to 5 cm (Table 1), while mainly gray and even black colors of sediments point to the sulfate reduction. The direct determinations of sulfide sulfur in the bottom deposits of deepwater station 4968 indicate that hydrotrolite as spots has been formed around organic detrital particles already in subsurface horizons.

The contents of phosphorus (0.01–8.5 μM in the pore water of the NZB, 0.1–35 μM in the shelf waters) and silica (90–371 μM and 131–499 μm, respectively) are different even at nearby stations (Table 1, Figs. 2-2 and 2-4). Maximum concentrations of phosphorus (up to 35 μM at st. 4974 and 6 μM at st. 4975) were found in the pore water of the surface sediments of the shelf. At the same time, the phosphorus contents in the surface waters of the axial deepwater station of the basin (st. 4968) are as low as 0.10–0.35 μM owing to the degradation of most plankton remains in the water column. For this reason, the phosphorus fluxes are directed from sediments to the bottom water on the shelf, where concentration of dissolved phosphates is less than 0.7 μM, and from seawater to the sediments on the basin floor. Another pattern is observed in the deeper sedimentary beds: the phosphate concentrations in pore water on the shelf, near the coast, decrease to almost zero values (st. 4575), increase (up to 8.52 μM per 50–58 cm) within the oxidized layer in the basin, and then unevenly decrease. Such heterogeneous phosphate distribution related to differences in depth, sediment composition, and the possible influence of zoobenthos (Table 1) may serve as the reason for the diagenetic circulation of the matter in sedimentary succession. A periodical influx of freshwater silica-rich biogenic material into the shelf zone serves as an additional silicon source in bottom sediments. The content of dissolved silicon in the pore water reaches the highest values in the surface shelf sediments (499 μM at station 4974), and shows an overall uneven decrease with depth, like the phosphorus content. Its lowest contents were found in the Pleistocene sediments of deepwater basin at a horizon of 223–232 cm. The highest concentrations in the surface layer provide stable flows of dissolved silicon from sediments into bottom water.

St. Anna Trench in the northern termination of Novaya Zemlya almost submeridionally links the Arctic Ocean (AO) and the Kara sea (Fig. 1), and reaches 550 m deep in the southern part. In terms of hydrology, biology, and geochemistry, the St. Anna Trench differs from the proper Kara sea, which is subjected to a strong effect of river runoff. It is separated from the NZB and the southern Kara Sea by a threshold around 100 m deep, above which two opposite currents occur: the SAT current directed from the Arctic to the south-

east along the western slope of the trench and the Eastern Novaya Zemlya (ENZ) current directed to the northeast [5]. Near the eastern termination of Novaya Zemlya, the currents diverge: the SAT turns to the northwest and returns back to the Arctic along the eastern slope of the trench, while the ENZ current runs further eastward. Both the currents are sufficiently intense (>50 cm/s), and their "turbulent" interaction leads to the formation of lenses, vortices, and filaments, which may provide the penetration and exchange of sedimentary matter, including plankton, between SAT and NZB. All the deepwater part of the SAT is filled with water of 35 PSU of Atlantic origin, with the vertical stirring of deepwater as the main mechanism of the differential–diffusion convection. The warmer (>1°C) and less saline surface water (34 PSU) is supplied with cyclonic current, which surrounds the trench along the slopes above the 200–300 m isobaths. Strong currents lead to the absence of mud deposits along the slopes and the appearance of sestonophages—animals feeding by suspension from water flow [5]. This is the coldest region of the Kara Sea, and its surface is devoid of ice only during two months per year. The core of the coldest water of the trench in the CTL is located at a depth of 150–200 m.

A frontal zone separating the river water influx from the south to north, which is accompanied by sharp depth gradients of hydrochemical parameters, is situated south of station 4988 (Fig. 1), approximately at 76° N. In the northern seaward part of the studied area (station 4983), chemical elements show even low-gradient distribution (Table 2) [10]. Such an important factor of sedimentation as the primary production (PP), which depends on the physical (salinity, temperature, transparency) and chemical parameters, sharply varies in the frontal zone. There are known concentrations of seawater-dissolved nutrients (3 μM nitrates, 0.5 μM phosphates, and (10 μM for silicon) that limit plankton production at low temperature [11]. Only the silicon content in the surface water of the southern part of the trench (station 4990, Table 2) is sufficient for its unlimited production. The integral PP decreases from almost 100 to 44.1 mg C/m^2 per day at station 4990, where salinity decreases owing to the propagation of desalinated waters of the Kara Sea. Note that the euphotic layer contains a significant amount of chl *a* (0.667 mg/m^3), which for low photosynthesis activity (assimilation numbers at lower temperatures decrease to 0.22 mg C/m chl per hour) does not lead to an increase of PP [11]. The low PP level of plankton limits bacterial production: the demand of bacteria for carbon is 2.3–7.7 times higher than algae-produced organic matter (OM) [16]. The concentrations of chemical components in the bottom water of SAT (Table 2) correspond to the characteristics of the Barents Sea waters.

Among other parameters of the water column are the extremely low contents of particulate matter, reaching less than 0.2–0.3 mg/L. According to optical data, the fluorescence intensity of chl *a* decreased by over 10 times, while that of dissolved organic matter (DOM) decreased by over 2 times as compared to the southern areas of the Kara Sea [2]. In the northern deepwater part of the SAT, the water has lower OM concentrations, which are close to its average content in the Arctic seas [1]. It was found that station 4983 is characterized by the lowest concentrations of dissolved organic matter (DOM) (0.94 and 0.84 mg C/L at depths of 61 and 200 m, respectively) and particulate organic carbon (POC) (17.2 μg C/L at 200 m) in the Kara Sea. At the same time, against the low particulate content in the surface layer, all SAT stations are characterized by elevated OM contents, reaching a maximum at station 4983 (43.9% C_{org} at particulate matter content of 0.23 mg/L). Due to the large distance of SAT from the OM sources and the low productivity of this region, this phenomenon seems strange, but suggests the autochthonous origin of OM [1]. At the same time, a more probable explanation would be the high "turbulence" in the region and the transfer of organic particulate matter from the NZB area. POC concentration in the bottom horizon is 106 μg C/ L, which suggests the existence of a nepheloid layer in the SAT [1].

The SAT extended from 77° N to 82° N is the main geophysical structure of the northwestern Kara Sea. This structure, being located between northern Novaya Zemlya, Franz Josef Land archipelago, and the North Kara Uplift, is fed by sedimentary influx from these structures, owing to coast abrasion, underground runoff, icemelt, and other sources, in general considered previously [13, 14]. The runoff of the Siberian rivers shows the minimum effect and only with respect to the fine pelitic material [7]. The bottom sediments of the SAT are represented by silty–pelitic muds with admixture of sand and even gravel, the fraction of which increases in the adjacent shelf areas (Table 1, Fig. 1). The studied sediments are ascribed to the marine Holocene with significant coarsening of sedimentary material in the lower parts of the studied cores (up to pebble at 2-m horizon of sediments, station 4983) at contact with the Upper Pleistocene. The SAT sediments are practically carbonate-free: $CaCO_3$ represented by only shelly bivalve detritus accounts for no more than 3% of the seafloor sediments, and less than 2% of the adjacent shelf sediments (Table 1). The kaolinite–chlorite–illite–smectite assemblage of clay minerals is predominant in this part of the trench [6] and, being the most reactive in the postsedimentation processes, plays a key role in the redistribution of manganese and iron during the early diagenesis.

Surface semiliquid bottom sediments in the southern part of SAT, in spite of the oxygen abundance in the suprabottom water, bear clear signs of reduction: brown–gray color and values of redox potential (E_{Pt} + 310 mV in 0–4 cm layer, station 4983, depth of 550 m, Table 1, Fig. 3). They are also saturated in zoobenthos and have high OM content (C_{org} 1.49%). Sediment rapidly becomes densely packed and clumpy, with the

appearance of ochreous inclusions (E_{Pt} + 150 mV) at 10 cm, an obvious sign of polychaete activity, which pump oxygen seawater in the lower parts of the surface layer. At a depth of 20 cm, sediment has maximum contents of iron (6.79%) and OM (C_{org} 1.67%), contains dark spots of hydrotroilite, the amount of which, judging from increasing patchiness, increases toward the center of the profile, and becomes gas-saturated (methane-filled cavities) [15]. Further downward, the light watered bed (179–184 cm) was identified with ochreous signs caused by advective feeding by oxygen water. The underlying very dense dark gray clay with inclusions of pebble obviously is indicative of change in sedimentation conditions from glacial–marine to marine ones [6, 7]. The previously expressed transformation of OM resulted in the presence and disappearance of brown color (MnO_2) in the surface horizons, the appearance of ochreous inclusions (FeOOH) in the deeper horizons, sulfate reduction (formation of dark hydrotroilite spots), and methane formation [15].

We believe that the most important factor of sedimentation and diagenesis in the southern SAT (station 4983) is the elevated OM content in sediments, reaching 1.4 according to our data and 2.1% C_{org} according to other data [1]. In our opinion, such a high OM influx under conditions of previously noted low PP and the large distance from coastal production may be provided by ENZ current, which contains pulsed ejecta (lenses) of waters with high or relatively high productivity from the southern Kara Sea [17], previously considered by us for the NZB. This provides a distribution of iron, manganese, and other chemical components related to the redox processes in the bottom sediments. Comprehensive consideration of sediment core from station 4983 gives more detailed insight into the geochemical features of the marine Holocene (last 10 ka) and preceding glacial–marine (Upper Pleistocene 13.3–10 ka) sedimentation stages. Based on core data from station 4983, the boundary between them lies at approximately 200 cm, where bottom deposits become coarser grained (pebbles), while C_{org} decreases to 0.5% (Table 1). Based on radiocarbon dating, this boundary is located at approximately 400 cm in the sediments of the southern stations of the trench and at 40 cm in the northern stations [6]. The iron content is 4.2–4.5% in the upper part of the core and decreases to less than 3% in the lower Pleistocene horizons. Note that the higher (6.8%) and lower (3.7%) iron contents in the adjacent horizons of the Holocene portion of the core may be explained by not only changes in the volumes of sedimentary influx, but also by the diagenetic redistribution of iron in the organic and gas-saturated sediments (20–90 cm), which also are characterized by the drop of iron content in pore water (4.9 mM). The diagenetic transition of manganese into solution against the background high OM content and its removal from sediment in the near-bottom water also result in a lower content of this element in the upper unit of sediments (0.04%). In pore water, only surface sediments show increase in Mn concentration (up to 22.6 μM), which is capable of providing manganese flux from sediments into bottom water. The latter concerns also fluxes of dissolved phosphorus and silicon from sediments owing to their much higher concentrations in the pore water of the surface bed of bottom sediments (4.0 and 320 μM, respectively) as compared to their concentrations in deep seawater (Tables 1, 2, Fig. 3).

The lower horizons of the redox layer are spanned by microbiological anaerobic processes of sulfate reduction and methane formation. However, under conditions of elevated OM content and inhomogeneity of sediments, especially, with respect to organic particles, these processes and, first of all, sulfate reduction, frequently, as already mentioned, begin in the surface horizons, at first in the "microniches" and are gradually propagated to the deeper horizons of sediment. In the bottom sediments of SAT, the intensity of sulfate reduction increases towards the center of the sedimentary profile up to 68.0 μg S dm^{-3} day^{-1} per 150–160 cm [15], while the content of reduced sulfur reaches 0.325%. This is the highest content of reduced sulfur, H_2S derivative (ΣS_{H_2S}), recorded by us in the Holocene deposits of the Kara Sea.

The methane cycle in the Kara Sea includes not only bottom sediments, but also water column, where bacterial methanogenesis (MG) proceeds on the particulate matter in the anaerobic microniches. In the bottom sediments of station 4983, MG is most completely expressed at horizons below 20–30 cm (Table 1), which underlie ochreous inclusions; generated methane forms cavities over the entire depth range of the Holocene unit with the maximum MG (256 nL CH_4 dm^{-3} day^{-1}) at the horizon of 80–90 cm [15]. It is pertinent to mention that such high indicators of microbiological activity were noted in the region of the lowest temperatures and biological productivity.

The geochemical features of bottom sediments in the shelf regions adjacent to SAT reflect both sedimentation in the deepwater part and the effect of boundary regions located south of station 4990. These are the soft brown muddy sediment at the surface, gradual compaction, clots and ochreous inclusions beneath them, blackening of the deeper horizons, the presence of silt beds, and the formation of very dense, almost dehydrated dark gray clays in the lower parts of the studied grounds (approximately at 100 cm, station 4988, Table 1). They are characterized by sharply decreased content of lithogenic elements (aluminum, iron, and manganese). Their elevated concentrations in pore water were found only in the upper horizons (Table 1). These obvious signs of transition to Pleistocene sediments in the upper part of the deposits almost completely disappear with distance from the trench (south of station 4990).

Contents of micrometals in the bottom sediments are very informative geochemical data (Table 3). Micrometals usually do not form their own mineral

Table 3. Metals in the bottom sediments of the Novaya Zemlya Basin and St. Anna Trench (10^{-4}%)

Sampling tool	Horizon, cm	Cu	Zn	Ni	Pb	Co	Cd	Cr
Novaya Zemlya Basin, in the area of Blagopoluchiya Bay								
Station 4968, depth of 360 m								
HC	0–1	27.4	84	47	21.8	9.6	0.74	123
	5–10	28.8	118	47	27.3	10.4	<0.05	149
	10–15	29.3	97	47	27.0	10.0	<0.05	94
	15–20	31.5	116	45	23.1	10.7	<0.05	138
	20–25	28.3	101	47	27.6	10.6	0.13	107
LDC	25–35	32.2	109	63	37.7	8.4	<0.05	77
	35–47	32.0	123	85	61.0	11.4	0.32	70
	50–58	27.9	106	68	32.7	7.8	<0.05	46
	82–86	47.0	125	65	28.2	14.0	0.31	83
	96–125	42.6	136	70	37.8	12.2	0.25	105
	141–153	48.0	110	59	34.1	14.0	0.21	110
	153–170	36.4	105	55	30.7	13.1	<0.05	110
	200–223	30.5	112	46	17.7	11.5	<0.05	97
	223–232	28.5	111	44	16.0	11.2	0.15	94
	272–304	19.9	74	40	16.6	9.5	<0.05	65
	324–345	25.8	80	38	14.4	9.6	0.14	73
Station 4974, depth of 170 m								
Bg	0–5	28.3	91	43	18.8	9.2	0.13	118
	5–10	27.0	94	40	15.2	8.3	0.20	125
	10–15	28.0	111	43	26.0	7.9	<0.05	160
LDC	10–15	27.8	100	40	19.2	9.4	<0.05	142
	25–32	30.0	94	39	14.4	8.8	<0.05	143
	32–61	31.2	64	40	13.9	4.7	0.15	142
	60–85	37.2	96	41	18.5	7.5	0.11	116
Station 4975, depth of 58 m								
Bg	0–5	25.7	107	33	12.8	6.5	<0.05	106
	5–10	24.6	78	32	12.0	6.6	<0.05	108
	10–15	26.0	89	33	12.6	7.5	0.14	119
LDC	10–24	26.3	83	35	12.9	7.7	0.06	123
	24–42	36.4	67	40	14.4	4.3	<0.05	120
	42–59	28.4	82	36	13.3	6.6	0.05	153
St. Anna Trench								
Station 4983, depth of 550 m								
HC	1–8	27.7	138	41	13.2	13.4	0.45	118
LDC	5–9	27.2	94	40	13.6	12.2	0.28	152
	9–13	27.4	91	40	13.3	11.7	0.30	142
	20–30	29.4	97	41	13.5	11.9	0.24	158
	80–90	26.5	90	40	14.0	11.0	0.44	174
	115–125	25.9	93	42	13.9	11.3	0.31	126
	150–160	25.8	96	39	14.2	10.7	0.25	139
	179–184	25.3	85	37	18.8	10.4	0.18	138
	184–206	18.6	56	25	11.9	8.5	0.17	139

Table 3. (Contd.)

Sampling tool	Horizon, cm	Cu	Zn	Ni	Pb	Co	Cd	Cr
Station 4988, depth of 180 m								
Bg	0–2	17.6	76	30.0	12.9	9.8	<0.05	112
	2–5	15.9	75	28.6	12.7	10.4	0.10	108
	5–10	17.2	80	35.6	12.1	10.7	0.03	128
LDC	10–22	15.2	61	24	13.1	8.4	0.17	104
	22–33	11.4	44	19.5	7.5	7.2	0.08	90
	33–45	16.5	61	26.8	12.7	9.7	0.10	115
	70–80	17.6	52	24.7	11.5	8.2	<0.05	98
	90–100	15.8	118	23.7	12.8	7.9	<0.05	98
	106–123	17.0	60	26.0	11.5	7.1	0.05	120
Station 4990, depth of 114 m								
HC	0–3	21.2	74	42.7	20.9	8.7	0.08	102
	3–8	25.2	88	45.5	17.7	11.4	0.31	155
	8–15	24.7	80	41.2	16.7	11.5	0.17	120
LDC	20–40	23.3	77	43.7	19.6	10.0	0.27	114
	40–105	27.3	83	44.5	18.5	10.9	0.30	142
	105–123	34.8	86	54.2	22.3	–	0.10	132
	123–170	37.6	90	55.0	22.4	10.3	<0.05	130
	170–186	34.8	80	54.5	25.6	9.1	<0.05	104
	196–206	18.8	57	26.5	11.4	10.0	<0.05	76
	206–216	17.5	48	22.5	10.0	8.9	0.13	68
	222–235	12.1	43	20.7	9.6	9.2	0.10	64

Al, Fe, and Mn are presented in Table 1.

phases in marine sediments, but are incorporated into structures of detrital and clay minerals, iron and manganese oxyhydroxides, or iron sulfides [3, 4] during sulfate reduction. However, if the content of reactive iron is insufficient to bind all H_2S formation during sulfate reduction, it remains in a free state, causing the characteristic smell of sediments. No free H_2S was found in the studied areas, unlike other regions of the Kara Sea [8].

The content of micrometals in the bottom sediments is characterized by significant scatter related to uneven sedimentary influx from different sources, as well as to the effect of postsedimentation oxidizing (ochreous films) or reducing (sulfate reduction) processes. The recorded intervals of concentrations (10^{-4}% as calculated for dry sediment of NZB, Table 3) account for 25–48 (50) for Cu, 67–107 (90) for Zn, 32–85 (70) for Ni, 12–61 (20) for Pb, 4–7 (10) for Co, <0.05–0.32 (0.8) for Cd, and 105–150 (90) for Cr; numbers in parentheses are the background concentrations for sedimentary rocks [4]. The corresponding intervals for SAT sediments are 11–37 for Cu, 43–56 for Zn, 18–25 for Ni, 10–26 for Pb, 8–12 for Co, <0.05–0.4 for Cd, and 64–174 for Cr.

A more detailed consideration of micrometals showed that the upper oxidized bed of the NZB bottom sediments is enriched in iron and manganese (Table 3, station 4968, 0–50 cm): Fe up to 9% and Mn up to 3%. Other components, especially Cu and Pb, are clearly confined to the underlying reduced sulfide-bearing sediments. The lower horizons assigned to the Upper Pleistocene (250–345 cm) have the lower contents of all studied metals. In the shelf sediments of areas adjacent to the NZB, the oxidized layer is significantly thinner (20 cm at station 4974 and 5 cm at station 4975), but shows no significant differences in the metal concentrations, except for Cu, which is confined to the reduced sulfide-bearing sediments (Tables 1 and 3).

The bottom sediments of SAT in the deepwater area (station 4983, depth of 550 m) contain a thinner oxidized bed (4 cm) as compared to that of NZB (50 cm), and have much lower concentrations of Fe and Mn (4.6 and 0.112%). In the underlying horizons (200 cm), the Fe and Mn contents decrease to 3 and 0.04%, respectively (Table 1). The contents of micrometals in the oxidized bed and in the lower horizons are also lower (Table 3), which may be explained by their lower influx due to the greater isolation of SAT from the Kara Sea as compared to NZB.

CONCLUSIONS

The northwestern deepwater basins of the Kara Sea, NZB and SAT, are far removed from the main sources of sedimentary material supplied by the Ob and Yenisei rivers. The frontal zone limited by the

southern slope of SAT hampers the penetration of freshened waters into the northern Kara Sea. The peculiarity of sedimentation in this area is determined by the complex and sufficiently active hydrodynamics of the Eastern Novaya Zemlya current supplied from the south and the SAT current bearing Arctic waters. In spite of the existence of the hydrodynamic frontal zone above the threshold separating the depression and trench, we cannot exclude the interaction of their water masses and exchange of sedimentary matters, including abrasion of the Novaya Zemlya coast, as well as the flora and fauna of the Kara Sea and Arctic. Hydrochemical features of the basins are characterized by differences not only in the surface and deep waters, especially with respect to oxygen and silica. Being ultraoligotrophic with respect to the biological productivity, the areas of the deepwater basins differ in the episodic drastic increase of production in the NZB and elevated influx of OM in the bottom sediments of SAT. The stratification of bottom sediments reflects not only a change in sedimentation mode in the upper Pleistocene and Holocene, but also the effect of diagenetic redox processes on the redistribution of chemical elements.

The most characteristic feature of the deepwater bottom sediments of the NZB in the Blagopoluchiya Bay area is the existence of an almost 50-cm surface oxidized bed enriched in manganese (up to 2.9%) and iron (up to 9.4%). This is provided by the closure of the deepwater part of the basin, which facilitates the preservation of these elements in the top sedimentary bed. Similar conditions are absent in the southern part of SAT, where the elevated content of OM leads to the release of manganese and, partly, iron, from sediments against the more active hydrodynamics of the near-bottom water and transfer of these elements in the water column.

ACKNOWLEDGMENTS

This work was supported by the Russian Foundation for Basic Research (project no. 13-05-00494) and the Russian Science Foundation (project no. 14-50-00095, materials processing).

REFERENCES

1. N. A. Belyaev, V. I. Peresypkin, and M. S. Ponyaev, "The organic carbon in the water, the particulate matter, and the upper layer of the bottom sediments of the west Kara Sea," Oceanology (Engl. Transl.) **50** (5), 706–715 (2010).
2. V. I. Burenkov, Y. A. Goldin, and M. D. Kravchishina, "The distribution of the suspended matter concentration in the Kara Sea in September 2007 based on ship and satellite data," Oceanology (Engl. Transl.) **50** (5), 798–805 (2010).
3. E. G. Gurvich, A. B. Isaeva, L. L. Demina, et al., "Chemical composition of bottom sediments of the Kara Sea and estuaries of Ob' and Yenisei rivers," Okeanologiya (Moscow) **34** (5), 766–775 (1994).
4. L. L. Demina, M. A. Levitan, and N. V. Politova, "Forms of some heavy metals in bottom sediments of the estuarial areas of the Ob' and Yenisei rivers," Geokhimiya, No. 2, 212–226 (2006).
5. A. G. Zatsepin, E. G. Morozov, A. N. Demidov, V. V. Kremenetskiy, S. G. Poyarkov, V. T. Paka, A. A. Kondrashov, A. O. Korzh, and D. M. Soloviev, "Circulation in the southwestern part of the Kara Sea in September 2007," Oceanology (Engl. Transl.) **50** (5), 643–656 (2010).
6. M. A. Levitan, Yu. A. Lavrushkin, and R. Stain, *Description of Sedimentation in the Arctic Ocean over Last 130 Kyr* (GEOS, Moscow, 2007) [in Russian].
7. M. A. Levitan, T. A. Khusid, V. M. Kuptsov, et al., "Types of the breaks of Upper Quaternary sediments in the Kara Sea," Okeanologiya (Moscow) **34** (5), 776–787 (1994).
8. A. Yu. Lein, Yu. M. Miller, B. B. Namsaraev, et al., "Biogeochemical processes of sulfur cycle at early diagenesis of sediments in profile of the Yenisei River – Kara Sea," Okeanologiya (Moscow) **34** (5), 681–692 (1995).
9. A. P. Lesitzin, V. P. Shevchenko, M. E. Vinogradov, et al., "Flows of sediments in the Kara Sea and estuaries of the Ob' and Yenisei rivers," Okeanologiya (Moscow) **34** (5), 748–758 (1994).
10. P. N. Makkaveev, P. A. Stunzhas, Z. G. Mel'nikova, P. V. Khlebopashev, and S. K. Yakubov, "Hydrochemical characteristics of the waters in the western part of the Kara Sea," Oceanology (Engl. Transl.) **50** (5), 688–697 (2010).
11. S. A. Mosharov, "Distribution of the primary production and chlorophyll a in the Kara Sea in September of 2007," Oceanology (Engl. Transl.) **50** (6), 884–892 (2010).
12. I. A. Nemirovskaya, "The concentration and composition of hydrocarbons in water, particulate matter, and bottom sediments of the Kara Sea," Oceanology (Engl. Transl.) **50** (5), 716–728 (2010).
13. A. G. Rozanov, V. A. Chechko, and N. M. Kokryatskaya, "The redox profile of the bottom sediments in the Ob River's mouth area," Oceanology (Engl. Transl.) **50** (5), 806–817 (2010).
14. A. G. Rozanov, "Geochemistry of the bottom sediments in the Kara Sea west of the Yamal Peninsula," Oceanology (Engl. Transl.) **55** (2), 263–272 (2015).
15. A. S. Savvichev, E. E. Zakharova, E. F. Veslopolova, I. I. Rusanov, M. V. Ivanov, and A. Y. Lein, "Microbial processes of the carbon and sulfur cycles in the Kara Sea," Oceanology (Engl. Transl.) **50** (6), 893–908 (2010).
16. A. F. Sazhin, N. D. Romanova, and S. A. Mosharov, "Bacterial and primary production in the pelagic zone of the Kara Sea," Oceanology (Engl. Transl.) **50** (5), 759–765 (2010).
17. I. N. Sukhanova, M. V. Flint, V. M. Sergeeva, and V. V. Kremenetskiy, "Phytoplankton of the south-western part of the Kara Sea," Oceanology (Engl. Transl.) **51** (6), 978–992 (2011).
18. M. V. Flint, "Cruise 54th of the research vessel *Akademik Mstislav Keldysh* in the Kara Sea," Oceanology (Engl. Transl.) **50** (5), 637–642 (2010).

Translated by M. Bogina